

Synthesis and Characterization of Two-Photon Chromophores Based on a Tetrasubstituted Tetraethynylethylene Scaffold

Tzu-Chau Lin,^{*,[a]} Yi-You Liu,^[a] May-Hui Li,^[a] Che-Yu Liu,^[a] Sheng-Yang Tseng,^[b]
Yu-Ting Wang,^[b] Ya-Hsin Tseng,^[b] Hui-Hsin Chu,^[b] and Chih-Wei Luo^[b]

Abstract: A new series of model dye molecules composed of three multi-branched analogues based on the tetrasubstituted tetraethynylethylene structural motif have been synthesized and experimentally shown to possess strong and widely dispersed two-photon absorption (2PA) in the near-IR region. It was found that the spectral position of the major 2PA band could be tuned

by the electronic nature of the selected substitution units. The studied model fluorophores also exhibited fairly low photodegradation of their fluorescence intensity even under prolonged UV-

light irradiation, which is beneficial for the development of fluorescence probes that are needed for long-term light exposure. Furthermore, representative chromophores were selected to demonstrate the power-control properties within the femtosecond and nanosecond time domains.

Keywords: absorption • chromophores • heterocycles • nonlinear optics • Sonogashira reaction

Introduction

The intrinsic quadratic dependence of two-photon absorption (2PA) on incident light intensity is one of the major characters that makes this third-order nonlinear optical phenomenon applicable in many photonics and biophotonics applications such as optical power limiting, frequency up-converted lasing, 3D optical data storage, 3D microfabrication, nondestructive bioimaging, and two-photon photodynamic therapy.^[1] For the development of two-photon technologies, the exploration of new materials with strong 2PA plays an equally important role as the advancement of high peak-power pulsed lasers. Through rational molecular design, it is possible to synthesize organic chromophores that exhibit several orders of intensified 2PA with other desired molecular characteristics simultaneously integrated, which helpfully compensates the relatively poor performance of commercialized dyes for the aforementioned applications based on 2PA. So far, it has been realized that the combination of several structural parameters such as intramolecular charge-transfer efficiency, effective size of the π -conjugation domain, and the structural dimensionality of

a molecule are closely related to molecular 2PA.^[2–10] This also means that the arrangement of the selected building units within a molecule plays a pivotal role in molecular design towards highly active 2PA chromophores. Following our continuous efforts in the search of effective structural parameters for the enhancement of molecular 2PA in multi-branched dye systems possessing heterocyclic ring complexes, in this paper we present the synthesis of new multipolar two-photon-active model chromophores based on the tetrasubstituted tetraethynylethylene (TEE) skeleton by using functionalized quinoxaline, indenoquinoxaline, and pyridopyrazine moieties as the substituents. We also report initial investigations into their nonlinear optical properties in both the femtosecond and nanosecond time domains.

Results

Model chromophores and synthesis

The chemical structures and the synthetic routes to the studied model compounds are illustrated in Figure 1 and Scheme 1, respectively. The compound set contained three multibranch analogues, the molecular structures of which were constructed by attaching four identical functionalized-quinoxalinoid lobes to a common central ethylene core through C=C bonds. Alternatively, the central part of these model compounds can be viewed as a TEE moiety, which is an attractive building unit for the construction of various π -conjugated carbon-rich structures that exhibit χ^3 nonlinearities and photochromic properties.^[11] Therefore, we believed that the 2PA-related properties of chromophores with an incorporated TEE skeleton deserved to be explored. In this work we tentatively introduced the TEE unit as the connection center and constructed a multipolar model chromo-

[a] Prof. T.-C. Lin, Y.-Y. Liu, M.-H. Li, C.-Y. Liu
Photonic Materials Research Laboratory
Department of Chemistry
National Central University
300 Jong-da Rd. 32001 Jhong-Li (Taiwan)
Fax: (+886)3-4227664
E-mail: tclin@ncu.edu.tw

[b] S.-Y. Tseng, Y.-T. Wang, Y.-H. Tseng, H.-H. Chu, Prof. C.-W. Luo
Department of Electrophysics
National Chiao-Tung University
Hsinchu (Taiwan)

Supporting information for this article is available on the WWW under <http://dx.doi.org/10.1002/asia.201402094>.

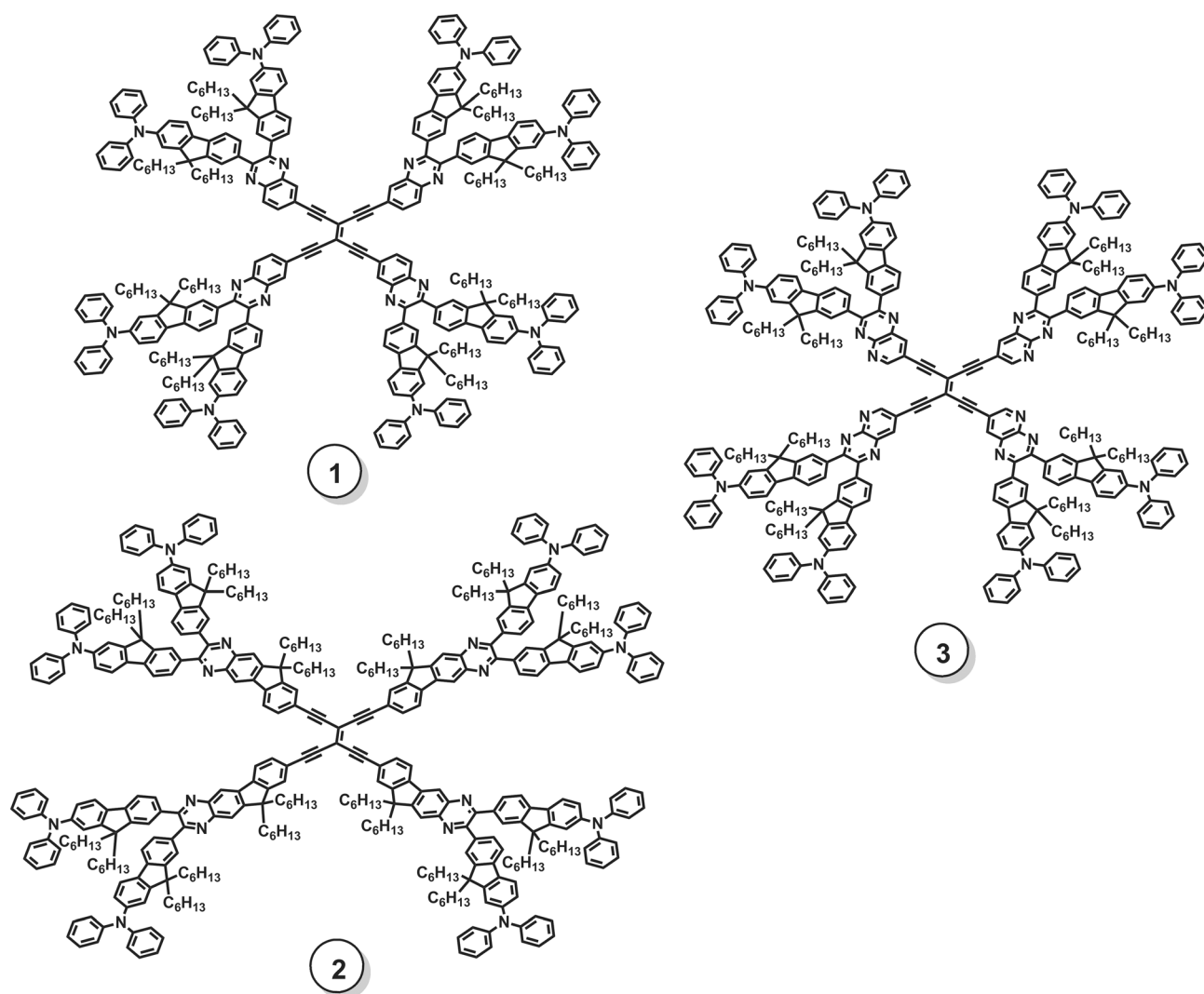


Figure 1. Molecular structures of the studied model chromophores.

phore system based on the tetrasubstituted TEE motif for the investigation of the 2PA-related properties. We selected quinoxalinoids as the major aryl substituents, as they were recently found to be useful structural units for building highly active 2PA dyes.^[10c-e,12] The model compounds were synthesized in acceptable yields by coupling terminal alkynes **10–12** with tetraiodoethylene under Sonogashira conditions, as illustrated in Scheme 1. The aforementioned terminal alkynes were obtained through consecutive functionalization starting from **4–6**, and the details of the syntheses of the precursors and targeted model compounds are described in the Experimental Section.

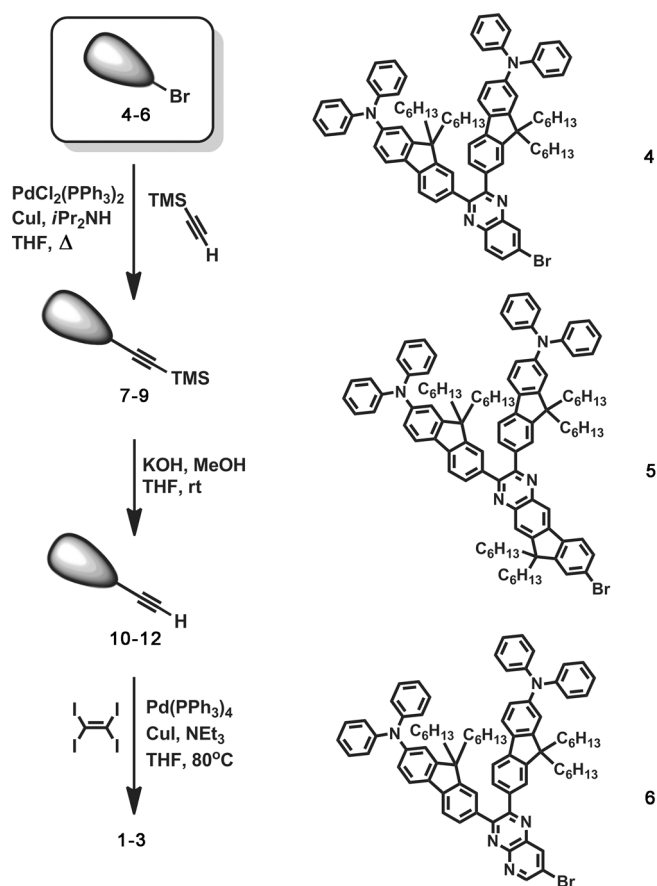
Linear and nonlinear optical properties

Linear absorption and fluorescence properties

Figure 2 illustrates the linear absorption and fluorescence spectra of the studied dye molecules in the solution phase by using toluene as the solvent. The studied model chromo-

phores displayed intense one-photon absorption (1PA) in the 300–470 nm range, and the lowest-energy absorption bands were located at 441 ($\epsilon \approx 1.63 \times 10^5$), 447 ($\epsilon \approx 2.76 \times 10^5$), and 470 nm ($\epsilon \approx 1.17 \times 10^5 \text{ cm}^{-1} \text{ M}^{-1}$) for **1**, **2**, and **3**, respectively. Solutions of these compounds also emitted intense fluorescence under irradiation of a common UV lamp with blue-greenish color for **1** and **2** and yellow-orange color for **3**, which is in agreement with the measured emission spectra (see Figure 2b).

Despite the symmetrical nature of their molecular structures, the fluorescence properties of all these model chromophores possessed strong solvent effects, including band positions and lifetimes as shown in Figure 3 by using chromophore **2** as a representative for this behavior. Similar behavior has been observed for other multipolar chromophore systems, and it is postulated that symmetry breaking owing to electron-vibration coupling and dipolar solvation effects are the major causes for this phenomenon.^[13,14] The measured photophysical properties of these model chromophores are collected in Table 1.



Scheme 1. Synthetic procedures for the target model chromophores.

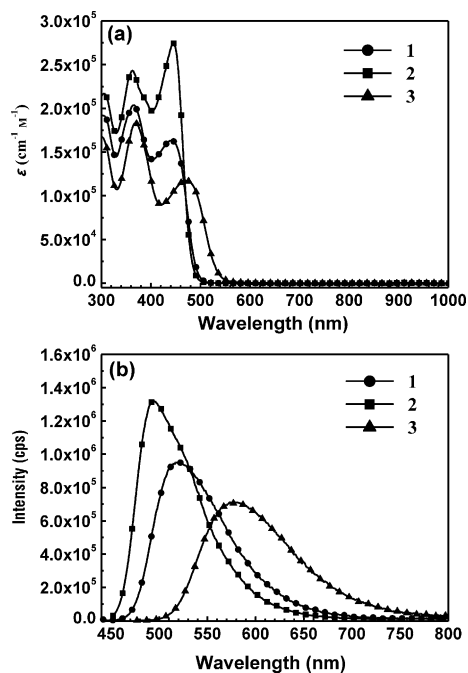


Figure 2. Linear absorption spectra (a) and fluorescence spectra (b) of 1–3 in the solution phase ($1 \times 10^{-6} \text{ M}$ in toluene).

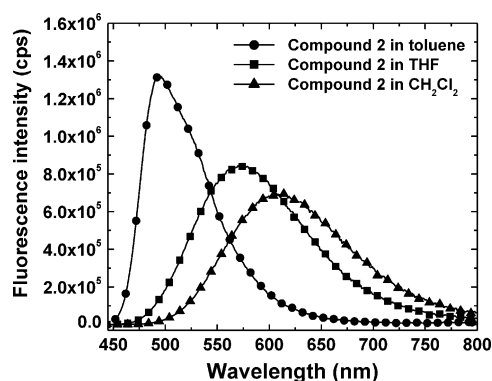


Figure 3. Fluorescence spectra of 2 in various solvents (concentration = $1 \times 10^{-6} \text{ M}$ for all cases). The measured fluorescence lifetime ($\tau_{\text{IPA-FL}}$) of 2 in toluene, THF, and CH_2Cl_2 was 1.5, 4.2, and 5.4 ns, respectively.

The photostability of the studied dye compounds in the solution phase ($1 \times 10^{-6} \text{ M}$ in toluene) was tentatively evaluated by continuously monitoring the decay of their fluorescence intensity over the course of UV irradiation. We utilized a set of UV lamps as the excitation light source to provide approximately 350 nm radiation with a total output of 64 W for this experiment. The detailed experimental arrangement is described in the Supporting Information. As illustrated in Figure 4, during the first 1 h of consecutive exposure to UV light, all of the model compounds retain $\geq 95\%$ of their original emission intensity. Prolonged irradiation further deteriorated the emissive properties of these model chromophore solutions. Compound 3 showed a larger fluorescence intensity drop ($\approx 22\%$), whereas this intensity drop was kept within approximately 9% for 1 and 2 after exposure to UV light for 3 h. Overall, model compounds 1 and 2 showed fairly good resistance to photodamage, and their resistance was superior to that of compound 3 under our experimental condition. We highly suspect that the weak photoresistance of 3 may originate from the pyridine unit in the ring complex, but clarification of this issue is currently beyond the scope of this work.

Two-photon-excited fluorescence properties

The studied model chromophores exhibited strong two-photon-excited fluorescence emission even under irradiation of an unfocused femtosecond laser beam at approximately 800 nm at a low-intensity level. Figure 5 illustrates the 2PA-induced fluorescence properties of the studied dye compounds measured by the two-photon-excited fluorescence (2PEF) technique. A wavelength-tunable mode-locked Ti:sapphire laser (Chameleon Ultra II, Coherent) that delivered approximately 140 fs pulses at a repetition rate of 80 MHz and a beam diameter of 2 mm was utilized as the excitation light source for these experiments. The intensity level of the excitation beam was carefully regulated to avoid absorption and photodegradation saturation of the samples during the course of the experiments. Furthermore, the relative position of the excitation beam was adjusted to be as close as possible to the wall of the quartz cell ($10 \times 10 \text{ mm}$ cuvette) so that only the emission from the front surface of

Table 1. Photophysical properties of model chromophores 1–3 in toluene.^[a]

Chromophore	$\lambda_{\text{max}}^{\text{abs}}$ [nm] ^[b]	$\log \epsilon$ ^[c]	$\lambda_{\text{max}}^{\text{em}}$ [nm] ^[d]	Φ_{f} ^[e]	$\tau_{2\text{PA-FL}}$ [ns] ^[f]	δ_2^{max} [GM] ^[g]	$\Phi_{\text{f}}\delta_2^{\text{max}}$ [GM] ^[h]
1	302	5.28	521	0.69	2.4	≈ 4280 (at 740 nm)	≈ 2950
	365	5.31					
	441	5.21					
2	306	5.34	496	0.66	1.5 (in toluene) 4.2 (in THF) 5.4 (in CH ₂ Cl)	≈ 8030 (at 750 nm)	≈ 5300
	361	5.39					
	447	5.44					
3	300	5.22	576	0.66	3.7	≈ 4000 (at 930 nm)	≈ 2640
	368	5.26					
	470	5.07					

[a] Concentration was 1×10^{-6} and 1×10^{-4} M for 1PA-related and 2PA-related measurements, respectively. [b] One-photon absorption maximum. [c] Molar absorption coefficient of the corresponding absorption band. [d] 1PA-induced fluorescence emission maximum. [e] Fluorescence quantum efficiency. [f] 2PA-induced fluorescence lifetime. [g] Maximum 2PA cross-section value (with experimental error $\pm 15\%$); $1 \text{ GM} = 1 \times 10^{-50} \text{ cm}^4 \text{ s} (\text{photon} \cdot \text{molecule})^{-1}$. [h] Two-photon action cross-section value.

Two-photon absorption spectra measurement

The dispersion of the 2PA behavior of these model molecules as a function of wavelength was probed in the near-IR regime (680–1000 nm) by the 2PEF method by using fluorescein ($\approx 80 \mu\text{M}$ in pH 11 NaOH solution) as the standard.^[15,16] Figure 6 shows the measured degenerate two-photon absorption spectra of these model compounds in toluene. From this figure one can see that all of these model compounds ex-

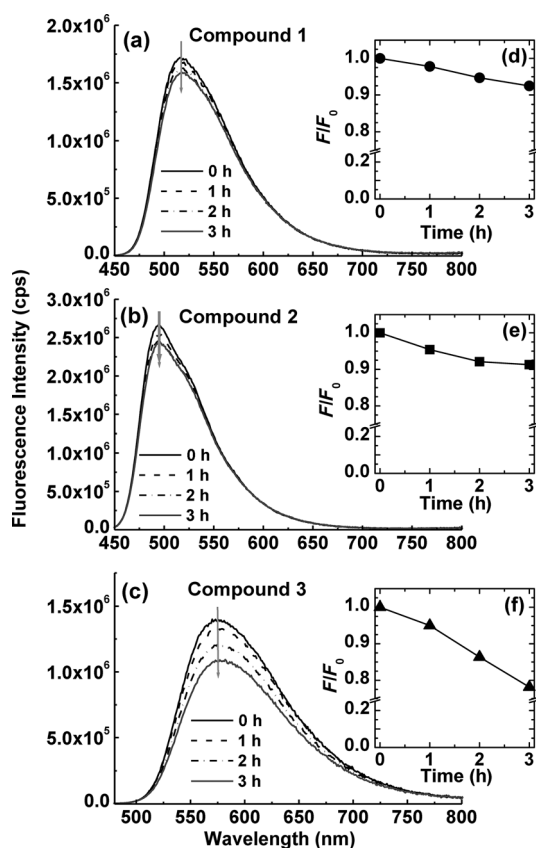


Figure 4. Evaluation of the photostability: Fluorescence spectra of the studied chromophores in the solution phase under consecutive irradiation of UV light at 350 nm (insets: fluorescence intensity change over the course of UV-light exposure).

the sample was recorded. Figure 5a illustrates the normalized 2PA-induced fluorescence spectra of 1–3 in the solution phase. The quadratic dependence of the fluorescence intensity on the excitation light intensity of these model compounds as shown in Figure 5b–d validates that 2PA is the major process that causes the observed up-converted emission.

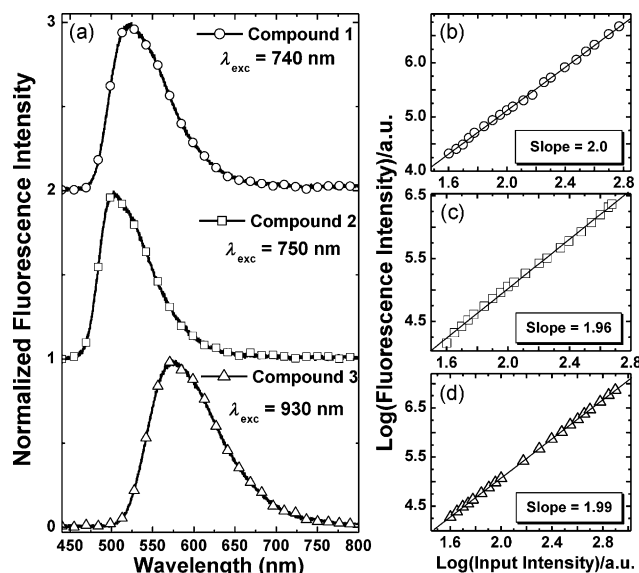


Figure 5. a) Two-photon-excited fluorescence spectra of the studied model chromophores; b–d) logarithmic plots of power-squared dependence of the 2PA-induced fluorescence intensity on the input intensity of these compounds in toluene.

hibited strong 2PA ($\geq 500 \text{ GM}$) within the major dynamic tuning range of a Ti:sapphire oscillator (i.e., 680–950 nm), which implies that the current structural combination based on attaching four electron-donor-functionalized quinoxalino-ids to a central TEE core is a useful approach toward strong 2PA dyes. To be more specific with regard to the 2PA spectral distribution of the studied model chromophores, compound 1 exhibited a broad 2PA band with two local maxima located at approximately 740 ($\delta_2 \approx 4280 \text{ GM}$) and 840 nm ($\delta_2 \approx 3920 \text{ GM}$), whereas compound 2 possessed a nearly identical 2PA dispersion pattern but with greatly elevated cross-section values, particularly at approximately 750 nm ($\delta_2 \approx 8030 \text{ GM}$), in comparison to 1, which indicates that the replacement of the quinoxaline unit by an indeno-

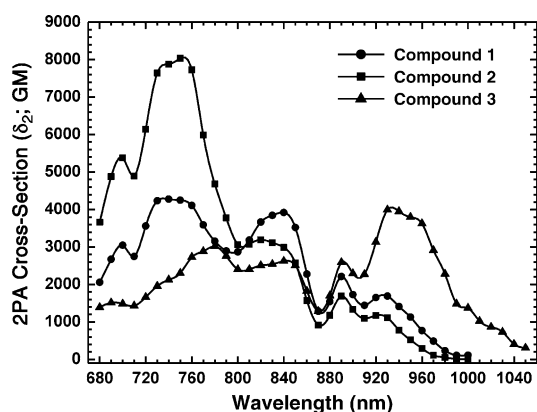


Figure 6. Measured degenerate two-photon absorption spectra of model chromophores **1–3** by the 2PEF method in toluene solution at 1×10^{-4} M (experimental error $\approx 15\%$).

quinoxaline moiety in this dye system had a positive effect on the promotion of molecular 2PA, especially at shorter wavelengths. This feature could become very desirable if large two-photon absorptivity within a specific spectral region is needed for particular applications. Compound **3** also showed widely dispersed 2PA and a bathochromically shifted local maximum at approximately 930 nm ($\delta_2 \approx 4000$ GM) compared to compound **1**.

Discussion of the results

From the measured photophysical properties of the studied model chromophores in the present work, the following features can be seen:

- 1) On the basis of the measured linear absorption spectra of the studied model chromophores by using compound **1** as a reference, compound **2** exhibited a distinct increase in the linear absorption with nearly identical spectral dispersion relative to compound **1**, whereas compound **3** showed relatively smaller linear absorption and a redshifted lowest-energy band. These features indicate that the involvement of a fluorene unit as part of the heterocyclic ring complex in this molecular system (as in the case of **2**) is an effective approach to enhance linear absorptivity without shifting the position of the absorption band, whereas utilization of a pyridine moiety for the construction of a heterocyclic ring complex (as in the case of **3**) is useful for expanding the spectral range of linear absorption by moving the lowest-energy band bathochromically.
- 2) Originally, we suspected that the TEE unit utilized as a ramification center in this model chromophore system could be photosensitive and consequently weaken the photostability of these compounds because of the ethynyl components in each structure; nevertheless, the experimental results revealed that this functional group is fairly inert toward UV radiation at approximately 350 nm. Among these three model compounds, **1** and **2** exhibited good photostability, which implies that the

structural units employed in these two compounds are suitable for the development of robust fluorescence probes that are needed for prolonged UV-light exposure. We are also aware that the results from the current photostability test may not fully represent the photoreistant character of these model compounds in other spectral regions, especially within their two-photon-active regime. Therefore, in addition to the presented work, a more comprehensive evaluation on the photostability of the studied chromophores under the exposure of near-IR radiation is needed, and such an experiment is one of the major subjects of our future work.

- 3) Relative to the 2PA of compound **1**, the noticeably hyperchromic 2PA of **2** in the shorter wavelength region and the distinctly redshifted 2PA of **3** indicate that fluorene can be an effective structural unit to enhance molecular 2PA with a roughly immobilized spectral position of the 2PA band, whereas the pyridine scaffold can efficiently redshift the 2PA and retain the same level of 2PA. These features are particularly useful for molecular design if either large 2PA at a specific spectral range or a redshifted 2PA band with a fixed cross-section level is required for different applications.
- 4) Recent theoretical studies on certain organic structures revealed that molecular 2PA is correlated to the square of the effective π -electron number.^[17] Although this approximation rule has not been verified yet to be totally suitable for various classes of conjugated molecules with different geometries, this scaling may serve as a reference for the tentative and qualitative analysis of our experimental results. From the viewpoint of molecular structure, the major difference between these model compounds is the heterocyclic part of each chromophore, and if it is assumed that the π -electrons on each model dye compound follow the same mode of contribution to the nonlinear response, the one with a ring complex that provides a larger number of π -electrons can be expected to exhibit a higher maximum molecular 2PA. Therefore, compound **2** can be expected to show the highest maximum molecular 2PA among the studied model compounds, as its indenoquinoxaline units provide the largest number of π -electrons compared to the π -electron numbers offered by the quinoxalines and pyridopyrazines on compounds **1** and **3**, respectively. In parallel, the maximum molecular 2PA cross-section values of compounds **1** and **3** can be expected to be at the same level, because the heterocyclic ring complex parts of these two compounds possess the same numbers of π -electrons.
- 5) Combining the medium-high fluorescence quantum yields and the 2PA cross-section values, chromophores **1–3** exhibit comparable maximum two-photon action cross-sections ($\Phi_F \delta_2^{\max}$, Φ_F is fluorescence quantum yield),^[1a–c,2a] and this property suggests that such a structural motif could be useful to build an efficient frequency up-converter for imaging-related applications such as two-photon-excited fluorescence microscopy. Additionally,

from the viewpoint of practical applications, it might be interesting to explore the photophysical properties of these model compounds in the solid state (e.g., in film configuration) and such work is currently being explored.

Optical power-limiting and stabilization properties in various time domains

Ideally, an optical limiter is expected to show spectrally broad and temporally agile response to incident laser light. Various nonlinear optical mechanisms have been employed to achieve optical limiting, and among them, 2PA is theoretically considered as a potential process to approach the aforementioned ideal characteristics for optical control. The quadratic dependence of 2PA on the input light intensity has made 2PA materials applicable in optical-limiting applications, because such materials are transparent to the incident light at low intensity but become opaque if the input intensity is increased. Given that this optical-control function stems from the intrinsic physical properties of the material, no external sensing or control mechanism is required to accomplish such optical suppression so that the response speed of a 2PA-based optical limiter can be very fast and the structure of the device can be very simple.

To demonstrate the 2PA-based power-limiting performance of the studied fluorophores, we selected compound **2** as a representative and utilized femtosecond laser pulses from a regenerative amplifier to probe its optical power-limiting properties at approximately 800 nm. The sample solution for this study was prepared in toluene with a concentration of 0.02 M, and the experimental setup for this measurement is described in detail in the Supporting Information. Figure 7 illustrates the measured data for the dependence of the output power on the input power of the probing laser beam. In this figure, the measured transmitted intensity data are presented by solid hexagons, and the dark-gray solid line is the theoretical curve, with the best fitting parameter of $\beta = 2.25 \text{ cm GW}^{-1}$. For comparison, the diagonal dotted line shows the behavior of a medium without nonlinear absorption, and one can see that the measured input–output curve starts to deviate from the linear transmission (diagonal dotted line) at low pumping power and rapidly approaches larger values of this deviation as the excitation power levels up. Moreover, the 2PA cross-section value of this model compound was calculated to be approximately 3100 GM from the performed optical-power-limiting experiment, which is very close to the result obtained from the 2PEF method within experimental uncertainty. This validates that 2PA should be the major cause for the observed up-converted emission and optical-power restriction in this chromophore system.

It has been reported that two-photon-active materials may also exhibit two-photon-assisted excited-state absorption (2PA-assisted ESA) under the irradiation of nanosecond or longer laser pulses, especially if the excited-state life-

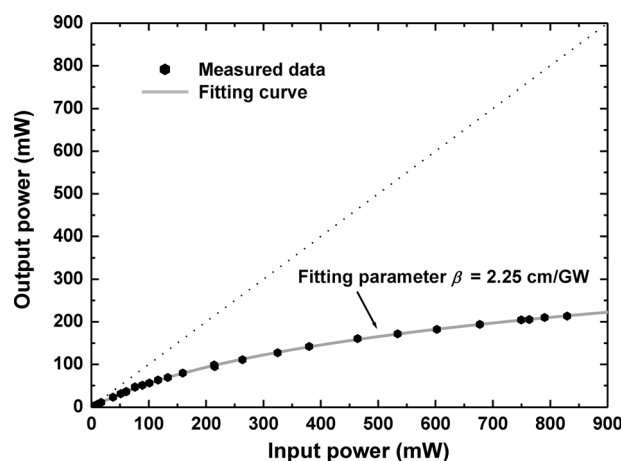


Figure 7. Measured output energy versus input energy of femtosecond laser pulses at 800 nm based on a 1 cm path solution sample of **2** in toluene at 0.02 M. The solid curve is the theoretical data with best-fit parameter of $\beta = 2.25 \text{ cm GW}^{-1}$.

time of the studied material is on the same time regime with the duration of the laser pulse.^[18] Such behavior will lead to larger apparent nonlinear attenuation of the incident light and consequently to better optical-control performance. From the viewpoint of fundamental research, it is important to gain knowledge of the connection between molecular structure and the 2PA-induced excited-state dynamics to establish a clear guideline for molecular design to precisely fulfill various requests of different applications. So far, only very limited experimental and theoretical attempts have been conducted to study 2PA-assisted ESA on the basis of organic dyes;^[18,19] therefore, the dependence of excited-state behavior on molecular structure is still lacking. Nevertheless, from the standpoint of applications, any medium that possesses large apparent nonlinear absorption over a wide spectral range could be very useful for effective optical-power attenuators against long laser pulses.^[20] These optical-power attenuation properties can also be utilized to suppress the power or energy fluctuation of laser pulses, which is very desirable for many laser-based applications such as optical telecommunication, optical fabrication, and optical data processing. To tentatively test the effective optical-power-stabilization properties against long laser pulses on the basis of these model compounds, chromophores **2** and **3** were selected for this experiment. Furthermore, given that the maxima 2PA of **2** and **3** are located at approximately 750 and 930 nm (see Figure 6), these two wavelengths were utilized for this test, because a higher 2PA-induced excited-state population could be reached and, consequently, larger apparent nonlinear absorption and better power-stabilization performance was expected. As an excitation light source, a tunable nanosecond laser system (an integrated Q-switched Nd:YAG laser and OPO: NT 342/3 from Ekspla) was employed to generate 6 ns laser pulses with controlled average pulse energy in the range from approximately 0.02 to 2 mJ with a repetition rate of 10 Hz for this investigation. The experimental results for the optical-stabilization study on the basis

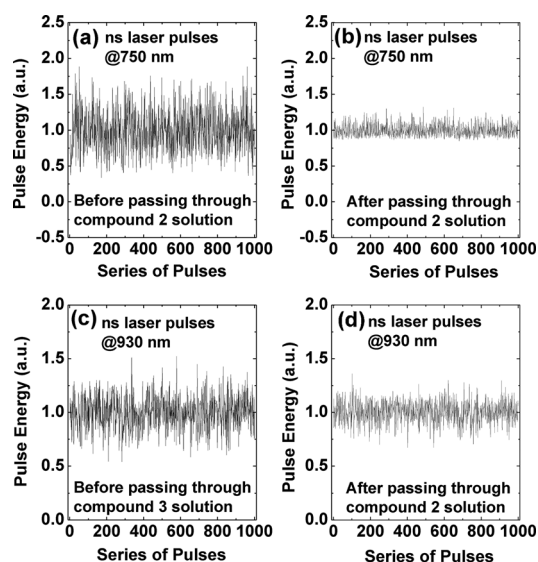


Figure 8. a,c) Measured instantaneous pulse energy fluctuation of the input laser pulses at 750 and ~930 nm; b,d) measured instantaneous pulse energy fluctuation of the output laser pulses at corresponding wavelengths after passing through solutions of **2** and **3**. The repetition rate of the laser pulse was 10 Hz, and the average input pulse energy level was approximately 1 mJ.

of these two sample solutions are shown in Figure 8. The curves in Figure 8a,c are the instantaneous pulse-energy changes in the incident laser beam at the corresponding wavelengths. The input pulses possess a relatively large energy fluctuation, as shown in Figure 8a,c, and after passing through solutions of **2** and **3**, reduced fluctuation of the pulse energy was observed for the output signals for each case, as illustrated in Figure 8b,d. For the purpose of comparison, the average levels of both the input and output signals were normalized to the same value, and from the measured data, compound **2** is a better optical-power stabilizer than compound **3**.

It should be reiterated that the individual contributions originating from intrinsic 2PA and possible ESA to the observed optical-energy attenuation of the tested chromophore systems is indistinguishable under the current experimental conditions. Therefore, the results presented herein could be assumed as a combined effect based on the aforementioned nonlinear processes.

Conclusions

In conclusion, we synthesized a novel multipolar chromophore set composed of three congeners on the basis of the tetrasubstituted tetraethynylethylene structural motif by using functionalized quinoxalinooids as the main aryl substituents. The initial experimental results showed that these model fluorophores display widely dispersed and strong two-photon absorption in the near-IR region. Tentative structure-2PA properties analysis revealed that integration of a fluorene unit as part of the heterocyclic ring complex

was a useful strategy to promote molecular 2PA, particularly at short wavelengths, whereas the incorporation of a pyridine moiety as a component of the heterocycles was beneficial in shifting the 2PA band bathochromically without a huge decline in the maximum 2PA. Moreover, model chromophore **2** was demonstrated to exhibit intrinsic 2PA-based optical-power-limiting properties against femtosecond laser pulses. In addition, both **2** and **3** were selected to test their optical-power stabilization properties against long laser pulses at wavelength positions for which these two model chromophores exhibit maximum 2PA, and as expected, fairly good power-stabilization performance of these two compounds was observed. Combining the good photostability and strong two-photon action cross-section ($\Phi_F \delta_2^{\max}$), these model chromophores could be potential prototypes for the development of 2PA-based fluorescence probes for long-term light exposure.

Experimental Section

General

All commercially available reagents for the preparation of the intermediates and targeted chromophores were purchased from Acros Organics or Alfa Aesar and were used as received, unless stated otherwise. ^1H NMR and ^{13}C NMR spectra were recorded with a 300 MHz spectrometer and referenced to tetramethylsilane or residual CHCl_3 . The representative numbering of carbon and hydrogen atoms on each intermediate and model chromophore for the assignment of the NMR signals was systematized and is illustrated in the Supporting Information. HRMS was conducted by using a Waters LCT ESI-TOF mass spectrometer. MALDI-TOF MS spectra were obtained with a Voyager DE-PRO mass spectrometer (Applied Biosystem, Houston, USA).

Photophysical methods

All of the linear optical properties of the subject model compound were measured by the corresponding spectrometers. Detailed experimental conditions as well as the optical setups for nonlinear optical properties investigations are described in the Supporting Information.

Synthesis

In Scheme 1, compounds **4–6** were the major starting materials for the synthesis of each intermediate and model chromophore. These three compounds were obtained by following established procedures.^[10c] For the synthesis of other key intermediates (i.e., compounds **7–9** and **10–12**) and targeted model compounds **1–3**, a series of functionalization steps starting from compounds **4–6** were conducted and are presented below. 7,7'-[6-[(Trimethylsilyl)ethynyl]quinoxaline-2,3-diyl]bis(9,9-dihexyl-*N,N*-diphenyl-9*H*-fluoren-2-amine) (**7**): $\text{PdCl}_2(\text{PPh}_3)_2$ (0.052 g, 0.074 mmol), CuI (0.023 g, 0.12 mmol), trimethylsilyl acetylene (0.18 g, 1.86 mmol), and *i* Pr_2NH (2.5 mL) were added to a mixture of **4** (1.5 g, 1.24 mmol) in dry THF (10 mL). The resulting solution was stirred at 90 °C under an Ar atmosphere for 21 h. After cooling to room temperature, H_2O (≈ 100 mL) was added to the reaction mixture. The above solution was then extracted with CH_2Cl_2 (3×30 mL), and the organic layer was collected and dried with $\text{MgSO}_4(6s)$. After removing the solvent, the crude product was purified by column chromatography on silica gel (THF/hexane=1:10) to give the final purified product as a yellow powder (1.4 g, 92.1%). ^1H NMR (300 MHz, CDCl_3): δ = 8.31 (s, 1H; H-F), 8.10–8.07 (d, J = 8.4 Hz, 1H; H-C), 7.78–7.76 (d, J = 8.4 Hz, 1H; H-B), 7.75–7.50 (m, 8H; H-9, H-12, H-13, H-15), 7.26–7.21 (m, 8H; H-2), 7.12–7.00 (m, 10H; H-3, H-6), 7.00–6.96 (m, 6H; H-1, H-8), 1.75–1.72 (m, 8H; H-f), 1.12–0.94 (m, 24H; H-c, H-d, H-e), 0.94–0.74 (m, 12H; H-a), 0.64 (s, 8H; H-b), 0.31 ppm (s, 9H; methyl hydrogen atoms of the TMS group);

¹³C NMR (75 MHz, CDCl₃, tentative assignments based on calculated values): δ = 154.62 (C-H), 154.22 (C-G), 152.61 (C-16), 150.59 (C-5), 150.51 (C-D), 147.87 (C-4), 147.50 (C-E), 141.80 (C-11), 140.80 (C-7), 140.70 (C-A), 137.05 (C-14), 135.39 (C-10), 132.67 (C-F), 132.54 (C-B), 129.13 (C-2), 128.98 (C-12, C-C), 124.34 (C-15), 123.86 (C-3), 123.34 (C-13), 122.55 (C-1), 120.86 (C-8), 118.91 (C-9), 118.82 (C-6), 104.39 (acetylene carbon), 97.12 (acetylene carbon), 55.05 (C-g), 40.09 (C-f), 31.53 (C-e), 29.56 (C-d), 23.82 (C-c), 22.59 (C-b), 14.06 (C-a), -0.11 ppm (methyl carbon atoms of the TMS group); HRMS (MALDI-TOF): *m/z*: calcd for C₈₇H₉₆N₄Si: 1224.7405 [M]⁺; found: 1224.7440.

7,7'-[10,10-Dihexyl-8-[(trimethylsilyl)ethynyl]-10H-indeno[1,2-g]quinoxaline-2,3-diyl]bis(9,9-dihexyl-*N,N*-diphenyl-9H-fluoren-2-amine) (**8**): PdCl₂(PPh₃)₂ (0.074 g, 0.10 mmol), CuI (0.03 g, 0.18 mmol), trimethylsilyl acetylene (0.29 g, 2.96 mmol), and *i*Pr₂NH (3 mL) were added to a mixture of **5** (2.58 g, 1.76 mmol) in dry THF (10 mL). The resulting solution was stirred at 90 °C under an Ar atmosphere for 17 h. After cooling to room temperature, H₂O (≈100 mL) was added to the reaction mixture. The above solution was then extracted with CH₂Cl₂ (3 × 30 mL), and the organic layer was collected and dried with MgSO_{4(6s)}. After removing the solvent, the crude product was purified by column chromatography on silica gel (THF/hexane = 1:10) to give the final purified product as an orange powder (2.4 g, 92%). ¹H NMR (300 MHz, CDCl₃): δ = 8.41 (s, 1H; H-H), 8.07 (s, 1H; H-K), 7.86–7.82 (d, *J* = 7.8 Hz, 1H; H-D), 7.62–7.58 (m, 10H; H-9, H-12, H-13, H-15, H-B, H-E), 7.27–7.21 (m, 8H; H-2), 7.12–7.07 (m, 10H; H-3, H-6), 7.04–6.98 (m, 6H; H-1, H-8), 2.19–2.01 (m, 4H; H-f'), 1.77–1.70 (m, 8H; H-f), 1.21–0.88 (m, 36H; H-c, H-c', H-d, H-d', H-e, H-e'), 0.81–0.63 (m, 30H; H-a, H-a', H-b, H-b'), 0.31 ppm (s, 9H; methyl hydrogen atoms of the TMS group); ¹³C NMR (75 MHz, CDCl₃, tentative assignments based on calculated values): δ = 153.46 (C-16), 153.03 (C-N), 152.58 (C-5), 151.24 (C-M), 150.57 (C-A), 150.48 (C-L), 147.89 (C-4), 147.40 (C-F), 143.15 (C-J), 141.52 (C-I), 141.36 (C-G), 141.19 (C-11), 140.06 (C-7), 137.52 (C-14), 137.44 (C-14'), 135.54 (C-10), 131.55 (C-B), 129.12 (C-2, C-12, C-E), 126.52 (C-D), 124.37 (C-15), 123.83 (C-3), 123.38 (C-K), 123.20 (C-C), 122.51 (C-1), 122.29 (C-13), 120.83 (C-6), 119.09 (C-9), 118.96 (C-8), 118.71 (C-H), 105.82 (acetylene carbon), 95.00 (acetylene carbon), 55.23 (C-g'), 55.04 (C-g), 41.37 (C-f'), 40.11 (C-f), 31.55 (C-e, C-e'), 29.71 (C-d'), 29.59 (C-d), 23.85 (C-c, C-c'), 22.61 (C-b, C-b'), 14.08 (C-a), 13.96 (C-a'), 0.01 ppm (methyl carbon atoms of the TMS group). HRMS (MALDI-TOF): *m/z*: calcd for C₁₀₆H₁₂₄N₄Si: 1480.9596 [M]⁺; found: 1480.9642.

7,7'-[7-[(Trimethylsilyl)ethynyl]pyrido[2,3-*b*]pyrazine-2,3-diyl]bis(9,9-dihexyl-*N,N*-diphenyl-9H-fluoren-2-amine) (**9**): PdCl₂(PPh₃)₂ (0.06 g, 0.09 mmol), CuI (0.03 g, 0.15 mmol), trimethylsilyl acetylene (0.22 g, 2.23 mmol), and *i*Pr₂NH (2.5 mL) were added to a mixture of **6** (1.80 g, 1.49 mmol) in dry THF (10 mL). The resulting solution was stirred at 90 °C under an Ar atmosphere for 24 h. After cooling to room temperature, H₂O (≈100 mL) was added to the reaction mixture. The above solution was then extracted with CH₂Cl₂ (3 × 30 mL), and the organic layer was collected and dried with MgSO_{4(6s)}. After removing the solvent, the crude product was purified by column chromatography on silica gel (THF/hexane = 1:10) to give the final purified product as an orange powder (1.53 g, 83.9%). ¹H NMR (300 MHz, CDCl₃): δ = 9.16–9.12 (d, *J* = 2.1 Hz, 1H; H-B), 8.58–8.54 (d, *J* = 2.1 Hz, 1H; H-E), 7.82–7.78 (d, *J* = 1.2 Hz, 1H; H-15), 7.71–7.14 (dd, *J* = 8.1, 1.2 Hz, 1H; H-12), 7.63–7.58 (d, *J* = 8.1 Hz, 1H; H-12'), 7.57–7.42 (m, 5H; H-13, H-13', H-9, H-9', H-15'), 7.31–7.21 (m, 8H; H-3), 7.15–7.07 (m, 10H; H-2, H-6), 7.07–6.97 (m, 6H; H-1, H-8), 1.82–1.61 (m, 8H; H-f, H-f'), 1.14–0.92 (m, 24H; H-c, H-c', H-d, H-d', H-e, H-e'), 0.81–0.75 (m, 12H; H-a, H-a'), 0.62 (s, 8H; H-b, H-b'), 0.33 ppm (s, 9H; methyl hydrogen atoms of the TMS group); ¹³C NMR (75 MHz, CDCl₃, tentative assignments based on calculated values): δ = 156.91 (C-G), 155.93 (C-F), 155.72 (C-B), 152.75 (C-16), 152.62 (C-16'), 150.71 (C-5), 150.55 (C-5'), 148.75 (C-C), 147.83 (C-4, C-4'), 147.71 (C-7, C-7'), 142.53 (C-11), 142.30 (C-11'), 139.97 (C-E), 136.49 (C-14), 136.08 (C-14'), 135.20 (C-10), 135.14 (C-10'), 134.95 (C-D), 129.72 (C-12), 129.14 (C-2, C-2'), 128.91 (C-12'), 124.45 (C-15), 124.31 (C-15'), 123.92 (C-3, C-3'), 123.29 (C-13, C-13'), 122.62 (C-1, C-1'), 121.18 (C-A), 120.99 (C-6), 120.93 (C-6'), 119.13 (C-9), 118.89 (C-8, C-8'), 118.56 (C-13'), 100.99 (acetylene carbon), 100.81 (acetylene carbon), 55.23 (C-g), 55.05 (C-g'), 40.18 (C-f), 40.05 (C-f'), 31.57 (C-e), 31.52 (C-e'), 29.54 (C-

d, C-d'), 23.84 (C-c), 23.77 (C-c'), 22.58 (C-b, C-b'), 14.06 (C-a, C-a'), -0.25 ppm (methyl carbon atoms on TMS group). HRMS (MALDI-TOF): *m/z*: calcd for C₈₆H₉₅N₄Si: 1226.8258 [M]⁺; found: 1226.8293.

7,7'-(6-Ethynylquinoxaline-2,3-diyl)bis(9,9-dihexyl-*N,N*-diphenyl-9H-fluoren-2-amine) (**10**): KOH (0.26 g, 4.57 mmol) was added to a mixture of **7** (1.4 g, 1.14 mmol) in THF/MeOH (5 mL/1 mL), and the resulting solution was stirred at RT under an Ar atmosphere for 15 h. Upon completion of the reaction, H₂O (≈100 mL) was added to the reaction mixture. The above solution was then extracted with CH₂Cl₂ (3 × 30 mL), and the organic layer was collected and dried with MgSO_{4(6s)}. After removing the solvent, the crude product was purified by column chromatography on silica gel (THF/hexane = 1:10) to give the final purified product as an orange powder (1.1 g, 83.4%). ¹H NMR (300 MHz, CDCl₃): δ = 8.35–8.34 (d, *J* = 1.2 Hz, 1H; H-F), 8.13–8.10 (d, *J* = 8.7 Hz, 1H; H-C), 7.80–7.77 (d, *J* = 8.7, 1.2 Hz, 1H; H-B), 7.59–7.50 (m, 8H; H-9, H-12, H-13, H-15), 7.27–7.21 (m, 8H; H-2), 7.12–7.08 (m, 10H; H-3, H-6), 7.08–6.98 (m, 6H; H-1, H-8), 3.27 (s, 1H; -C≡H), 1.74 (s, 8H; H-f), 1.13–0.94 (m, 24H; H-c, H-d, H-e), 0.86–0.76 (m, 12H; H-a), 0.64 ppm (s, 8H; H-b); ¹³C NMR (75 MHz, CDCl₃, tentative assignments based on calculated values): δ = 154.79 (C-G), 154.50 (C-H), 152.63 (C-16), 150.60 (C-5), 147.88 (C-4), 147.54 (C-D, C-E), 141.88 (C-11), 140.95 (C-7), 140.62 (C-A), 136.97 (C-14), 135.35 (C-10), 133.07 (C-F), 132.48 (C-B), 129.15 (C-2), 129.00 (C-12, C-C), 124.35 (C-15), 123.88 (C-3), 123.33 (C-13), 122.57 (C-1), 120.89 (C-8), 119.01 (C-9, C-6), 83.07 (acetylene carbon), 79.55 (acetylene carbon), 55.07 (C-g), 40.09 (C-f), 31.53 (C-e), 29.57 (C-d), 23.83 (C-c), 22.60 (C-b), 14.08 ppm (C-a). HRMS (MALDI-TOF): *m/z*: calcd for C₈₄H₈₈N₄: 1152.7009 [M]⁺; found: 1152.7042.

7,7'-(8-Ethynyl-10,10-dihexyl-10H-indeno[2,1-g]quinoxaline-2,3-diyl)-bis(9,9-dihexyl-*N,N*-diphenyl-9H-fluoren-2-amine) (**11**): KOH (0.27 g, 4.85 mmol) was added to a mixture of **8** (2.4 g, 1.62 mmol) in THF/MeOH (10 mL/2 mL), and the resulting solution was stirred at RT under an Ar atmosphere for 5 h. Upon completion of the reaction, H₂O (≈100 mL) was added to the reaction mixture. The above solution was then extracted with CH₂Cl₂ (3 × 30 mL), and the organic layer was collected and dried with MgSO_{4(6s)}. After removing the solvent, the crude product was purified by column chromatography on silica gel (THF/hexane = 1:10) to give the final purified product as an orange powder (2.1 g, 92%). ¹H NMR (300 MHz, CDCl₃): δ = 8.44 (s, 1H; H-H), 8.10 (s, 1H; H-K), 7.89–7.86 (d, *J* = 7.8 Hz, 1H; H-D), 7.63–7.52 (m, 10H; H-9, H-12, H-13, H-15, H-B, H-E), 7.27–7.22 (m, 8H; H-2), 7.14–7.09 (m, 10H; H-3, H-6), 7.03–6.99 (m, 6H; H-1, H-8), 3.20 (s, 1H; -C≡H), 2.13–2.02 (m, 4H; H-f'), 1.84–1.74 (m, 8H; H-f), 1.11–1.04 (m, 36H; H-c, H-c', H-d, H-d', H-e, H-e'), 0.86–0.66 ppm (m, 30H; H-a, H-a', H-b, H-b'); ¹³C NMR (75 MHz, CDCl₃, tentative assignments based on calculated values): δ = 153.48 (C-16), 153.40 (C-16'), 153.11 (C-N), 152.58 (C-5), 151.34 (C-M), 150.58 (C-A), 150.50 (C-L), 147.89 (C-4), 147.41 (C-F), 143.00 (C-J), 141.54 (C-I), 141.39 (C-G), 141.16 (C-11), 140.35 (C-7), 137.49 (C-14), 137.41 (C-14'), 135.52 (C-10), 131.56 (C-B), 129.12 (C-2, C-12), 128.92 (C-E), 126.79 (C-D), 124.36 (C-15), 123.83 (C-3), 123.37 (C-K), 122.52 (C-1), 122.35 (C-13), 122.14 (C-C), 120.90 (C-6), 120.82 (C-6'), 119.08 (C-9), 118.96 (C-8), 118.90 (C-8'), 118.82 (C-H), 84.35 (acetylene carbon), 77.92 (acetylene carbon), 55.23 (C-g), 55.04 (C-g), 41.32 (C-f'), 40.11 (C-f), 31.54 (C-e, C-e'), 29.67 (C-d'), 29.58 (C-d), 23.84 (C-c, C-c'), 22.61 (C-b), 22.55 (C-b'), 14.07 (C-a), 13.94 ppm (C-a'). HRMS (MALDI-TOF): *m/z*: calcd for C₁₀₃H₁₁₆N₄: 1408.9200 [M]⁺; found: 1408.9240.

7,7'-(7-Ethynylpyrido[2,3-*b*]pyrazine-2,3-diyl)bis(9,9-dihexyl-*N,N*-diphenyl-9H-fluoren-2-amine) (**12**): KOH (0.28 g, 4.99 mmol) was added to a mixture of **9** (1.53 g, 1.24 mmol) in THF/MeOH/H₂O (10 mL/5 mL/1 mL), and the resulting solution was stirred at RT under an Ar atmosphere for 2 h. After cooling to room temperature, H₂O (≈100 mL) was added to the reaction mixture. The above solution was then extracted with CH₂Cl₂ (3 × 30 mL), and the organic layer was collected and dried with MgSO_{4(6s)}. After removing the solvent, the crude product was purified by column chromatography on silica gel (THF/hexane = 1:10) to give the final purified product as an orange powder (1.1 g, 76.3%). ¹H NMR (300 MHz, CDCl₃): δ = 9.16–9.15 (d, *J* = 2.1 Hz, 1H; H-B), 8.61–8.60 (d, *J* = 2.1 Hz, 1H; H-E), 7.81 (s, 1H; H-15), 7.71–7.68 (d, *J* = 8.1 Hz, 1H; H-

12), 7.64–7.58 (d, $J=7.8$ Hz, 1H; H-12'), 7.59–7.43 (m, 5H; H-13, H-13', H-9, H-9', H-15'), 7.27–7.21 (m, 8H; H-2), 7.20–7.10 (m, 10H; H-3, H-6), 7.08–6.98 (m, 6H; H-1, H-8), 3.42 (s, 1H; $-\text{C}\equiv\text{H}$), 1.81–1.68 (m, 8H; H-f, H-f'), 1.26–1.02 (m, 24H; H-c, H-c', H-d, H-d', H-e, H-e'), 0.92–0.78 (m, 12H; H-a, H-a'), 0.77–0.75 ppm (m, 8H; H-b, H-b'); ^{13}C NMR (75 MHz, CDCl_3 , tentative assignments based on calculated values): $\delta=157.25$ (C-G), 156.09 (C-F), 155.56 (C-B), 152.76 (C-16), 152.62 (C-16'), 150.75 (C-5), 150.56 (C-5'), 148.99 (C-C), 147.81 (C-4, C-4'), 142.62 (C-7, C-7'), 142.38 (C-11, C-11'), 140.60 (C-E), 136.38 (C-14), 135.97 (C-14'), 135.13 (C-10, C-10'), 134.83 (C-D), 129.73 (C-12), 129.15 (C-2, C-2'), 128.90 (C-12'), 124.45 (C-15), 124.28 (C-15'), 123.93 (C-3, C-3'), 123.27 (C-13, C-13'), 122.64 (C-1, C-1'), 121.01 (C-6, C-6'), 120.09 (C-A), 119.19 (C-9), 118.86 (C-8, C-8'), 118.56 (C-9'), 82.57 (acetylene carbon), 79.97 (acetylene carbon), 55.24 (C-g), 55.06 (C-g'), 40.17 (C-f), 40.05 (C-f'), 31.57 (C-e), 31.51 (C-e'), 29.54 (C-d, C-d'), 23.85 (C-c, C-c'), 22.58 (C-b, C-b'), 14.05 ppm (C-a, C-a'). HRMS (MALDI-TOF): m/z : calcd for $\text{C}_{83}\text{H}_{87}\text{N}_5$; 1153.6962 $[M]^+$; found: 1153.6965.

Compound 1: Pd(PPh₃)₄ (0.015 g, 0.011 mmol), CuI (3 mg, 0.011 mmol), tetraiodoethene (0.12 g, 0.23 mmol), and NEt₃ (3 mL) were added to a mixture of **10** (1.1 g, 0.95 mmol) in THF (10 mL). The resulting solution was stirred at 90 °C under an Ar atmosphere for 26 h. After cooling to room temperature, H₂O (≈100 mL) was added to the reaction mixture. The above solution was then extracted with CH₂Cl₂ (3 × 30 mL), and the organic layer was collected and dried with MgSO_{4(s)}. After removing the solvent, the crude product was purified by column chromatography on silica gel (THF/hexane=1:10) to give the final purified product as a yellow powder (0.6 g, 57.1 %). ^1H NMR (300 MHz, CDCl_3): $\delta=8.43$ – 8.42 (d, $J=1.2$ Hz, 4H; H-F), 8.16–8.13 (d, $J=8.7$ Hz, 4H; H-C), 7.86–7.82 (d, $J=8.7$, 1.2 Hz, 4H; H-B), 7.60–7.50 (m, 32H; H-9, H-12, H-13, H-15), 7.27–7.21 (m, 32H; H-2), 7.13–7.09 (m, 40H; H-3, H-6), 7.03–6.99 (m, 24H; H-1, H-8), 1.76–1.74 (m, 32H; H-f), 1.14–1.04 (m, 96H; H-c, H-d, H-e), 0.82–0.76 (m, 48H; H-a), 0.65 ppm (s, 32H; H-b); ^{13}C NMR (75 MHz, CDCl_3 , tentative assignments based on calculated values): $\delta=155.00$ (C-H), 154.67 (C-G), 152.64 (C-16), 150.64 (C-5), 150.58 (C-5'), 147.86 (C-4), 147.56 (C-E), 141.99 (C-11), 141.93 (C-D), 141.30 (C-7), 140.64 (C-A), 136.88 (C-14), 135.31 (C-10), 133.74 (C-F), 132.48 (C-B), 129.42 (C-C), 129.14 (C-2), 129.04 (C-12), 124.35 (C-15), 123.89 (C-3), 123.32 (C-13), 122.70 (ethylene carbon atoms), 122.58 (C-1), 120.90 (C-8), 118.97 (C-9, C-6), 82.22 (acetylene carbon atoms), 76.16 (acetylene carbon atoms), 55.07 (C-g), 40.08 (C-f), 31.53 (C-e), 29.56 (C-d), 23.83 (C-c), 22.60 (C-b), 14.07 ppm (C-a). HRMS (MALDI-TOF): m/z : calcd for $\text{C}_{338}\text{H}_{348}\text{N}_6$; 4635.6206 $[M]^+$; found: 4635.6372.

Compound 2: Pd(PPh₃)₄ (0.02 g, 0.018 mmol), CuI (3.37 mg, 0.018 mmol), tetraiodoethene (0.19 g, 0.35 mmol), and NEt₃ (3.6 mL) were added to a mixture of **11** (2.1 g, 1.48 mmol) in THF (12 mL). The resulting solution was stirred at 90 °C under an Ar atmosphere for 12 h. After cooling to room temperature, H₂O (≈100 mL) was added to the reaction mixture. The above solution was then extracted with CH₂Cl₂ (3 × 30 mL), and the organic layer was collected and dried with MgSO_{4(s)}. After removing the solvent, the crude product was purified through column chromatography on silica gel (THF/hexane=1:10) to give the final purified product as an orange powder (1.1 g, 55 %). ^1H NMR (300 MHz, CDCl_3): $\delta=8.46$ (s, 4H; H-H), 8.11 (s, 4H; H-K), 7.92–7.89 (d, $J=7.8$ Hz, 4H; H-D), 7.65–7.52 (m, 40H; H-9, H-12, H-13, H-15, H-B, H-E), 7.27–7.22 (m, 32H; H-2), 7.13–7.09 (m, 40H; H-3, H-6), 7.03–6.98 (m, 24H; H-1, H-8), 2.14–2.11 (m, 16H; H-f'), 1.76–1.74 (m, 32H; H-f), 1.13–1.04 (m, 144H; H-c, H-c', H-d, H-d', H-e, H-e'), 0.82–0.68 ppm (m, 120H; H-a, H-a', H-b, H-b'); ^{13}C NMR (75 MHz, CDCl_3 , tentative assignments based on calculated values): $\delta=153.57$ (C-16), 153.44 (C-16'), 153.23 (C-N), 152.60 (C-5), 151.49 (C-M), 150.60 (C-A), 150.53 (C-L), 147.91 (C-4), 147.43 (C-F), 142.84 (C-J), 141.59 (C-I), 141.54 (C-G), 141.49 (C-C), 141.18 (C-11), 140.86 (C-7), 137.47 (C-14), 137.39 (C-14'), 135.53 (C-10), 131.97 (C-B), 129.13 (C-2, C-12), 128.92 (C-E), 127.24 (C-D), 124.37 (C-15), 123.85 (C-3), 123.39 (C-K), 122.53 (C-1), 121.80 (ethylene carbon atoms), 121.14 (C-13), 120.83 (C-6), 119.10 (C-9, C-8, C-H), 83.21 (acetylene carbon atoms), 74.98 (acetylene carbon atoms), 55.29 (C-g'), 55.06 (C-g), 41.33 (C-f'), 40.12 (C-f), 31.55 (C-e, C-e'), 29.69 (C-d'), 29.59 (C-d), 23.85 (C-c, C-c'), 22.62 (C-b, C-b'), 14.08 (C-a), 13.96 ppm (C-a'). HRMS (MALDI-TOF): m/z : calcd for $\text{C}_{414}\text{H}_{460}\text{N}_{16}$; 5660.3447 $[M]^+$; found: 5660.3721.

Compound 3: Pd(PPh₃)₄ (0.013 g, 0.011 mmol), CuI (2.16 mg, 0.011 mmol), tetraiodoethene (0.12 g, 0.22 mmol), and NEt₃ (2.5 mL) were added to a mixture of **12** (1.1 g, 0.95 mmol) in THF (10 mL). The resulting solution was stirred at 90 °C under an Ar atmosphere for 18 h. After cooling to room temperature, H₂O (≈100 mL) was added to the reaction mixture. The above solution was then extracted with CH₂Cl₂ (3 × 30 mL), and the organic layer was collected and dried with MgSO_{4(s)}. After removing the solvent, the crude product was purified by column chromatography on silica gel (THF/hexane=1:10) to give the final purified product as a red powder (0.5 g, 47.6 %). ^1H NMR (300 MHz, CDCl_3): $\delta=9.23$ – 9.22 (d, $J=2.1$ Hz, 4H; H-B), 8.70–8.69 (d, $J=2.1$ Hz, 4H; H-E), 7.83 (s, 4H; H-15), 7.73–7.70 (dd, $J=8.1$, 1.2 Hz, 4H; H-12), 7.70–7.63 (d, $J=8.1$ Hz, 4H; H-12'), 7.60–7.57 (d, $J=8.1$ Hz, 8H; H-13, H-13'), 7.52–7.48 (d, $J=8.1$ Hz, 4H; H-9), 7.48–7.44 (m, 8H; H-9', H-15'), 7.27–7.22 (m, 32H; H-2), 7.13–7.08 (m, 40H; H-3, H-6), 7.03–6.99 (m, 24H; H-1, H-8), 1.84–1.69 (m, 32H; H-f, H-f'), 1.15–1.03 (m, 96H; H-c, H-c', H-d, H-d', H-e, H-e'), 0.93–0.76 (m, 48H; H-a, H-a'), 0.63 ppm (s, 32H; H-b, H-b'); ^{13}C NMR (75 MHz, CDCl_3 , tentative assignments based on calculated values): $\delta=157.48$ (C-G), 156.33 (C-F), 155.40 (C-B), 152.73 (C-16), 152.57 (C-16'), 150.71 (C-5), 150.54 (C-5'), 149.17 (C-C), 147.74 (C-4, C-4'), 142.76 (C-7), 142.46 (C-11), 141.08 (C-E), 136.21 (C-14), 135.79 (C-14'), 134.99 (C-10, C-A), 134.67 (C-D), 129.75 (C-12), 129.10 (C-2), 124.42 (C-15), 124.21 (C-15'), 123.90 (C-3), 123.20 (C-13), 122.61 (C-1), 121.01 (C-6), 119.27 (C-9), 119.18 (ethylene carbon atoms), 118.76 (C-8), 118.56 (C-9'), 79.95 (acetylene carbon atoms), 78.38 (acetylene carbon atoms), 55.19 (C-g), 55.01 (C-g'), 40.09 (C-f), 31.51 (C-e), 31.50 (C-e'), 29.48 (C-d), 23.79 (C-c), 22.53 (C-b), 14.01 ppm (C-a).

Acknowledgements

We thank the National Science Council (NSC), Taiwan for financial support through grant number 101-2113M-008-003-MY2.

- a) S. Yao, K. D. Belfield, *Eur. J. Org. Chem.* **2012**, 3199–3217; b) M. Pawlicki, H. A. Collins, R. G. Denning, H. L. Anderson, *Angew. Chem. Int. Ed.* **2009**, *48*, 3244–3266; *Angew. Chem.* **2009**, *121*, 3292–3316; c) H. M. Kim, B. R. Cho, *Acc. Chem. Res.* **2009**, *42*, 863–872; d) M. Rumi, S. Barlow, J. Wang, J. W. Perry, S. R. Marder, *Advances in Polymer Science Vol. 213: Photoresponsive Polymers I* (Eds.: S. R. Marder, K.-S. Lee), **2008**, Springer, Berlin, pp. 1–95; e) K. D. Belfield, S. Yao, M. V. Bondar, *Advances in Polymer Science Vol. 213: Photoresponsive Polymers I* (Eds.: S. R. Marder, K.-S. Lee), **2008**, Springer, Berlin, pp. 97–156; f) G. S. He, L.-S. Tan, Q. Zheng, P. N. Prasad, *Chem. Rev.* **2008**, *108*, 1245–1330; g) T.-C. Lin, S.-J. Chung, K.-S. Kim, X. Wang, G. S. He, J. Swiatkiewicz, H. E. Pudav, P. N. Prasad, *Advances in Polymer Science Vol. 161: Polymers for Photonics Applications II* (Ed.: K.-S. Lee), **2003**, Springer, Berlin, pp. 157–193; h) C. W. Spangler, *J. Mater. Chem.* **1999**, *9*, 2013–2020; i) Q. Zheng, H. Zhu, S.-C. Chen, C. Tang, E. Ma, X. Chen, *Nat. Photonics* **2013**, *7*, 234–239.
- a) H. M. Kim, B. R. Cho, *Chem. Commun.* **2009**, 153–164; b) F. Terenziani, C. Katan, E. Badaeva, S. Tretiak, M. Blanchard-Desce, *Adv. Mater.* **2008**, *20*, 4641–4678.
- a) M. Albota, D. Beljonne, J.-L. Brédas, J. E. Ehrlich, J.-Y. Fu, A. A. Heikal, S. E. Hess, T. Kogej, M. D. Levin, S. R. Marder, D. McCord-Maughon, J. W. Perry, H. Rockel, M. Rumi, G. Subramaniam, W. W. Webb, X.-L. Wu, C. Xu, *Science* **1998**, *281*, 1653–1656; b) M. Rumi, J. E. Ehrlich, A. A. Heikal, J. W. Perry, S. Barlow, Z. Hu, D. McCord-Maughon, T. C. Parker, H. Röel, S. Thayumanavan, S. R. Marder, D. Beljonne, J.-L. Brédas, *J. Am. Chem. Soc.* **2000**, *122*, 9500–9510.
- a) L. Porrès, C. Katan, O. Mongin, T. Pons, J. Mertz, M. Blanchard-Desce, *J. Mol. Struct.* **2004**, *704*, 17–24; b) L. Porrès, O. Mongin, C. Katan, M. Charlot, T. Pons, J. Mertz, M. Blanchard-Desce, *Org. Lett.* **2004**, *6*, 47–50; c) C. Katan, F. Terenziani, O. Mongin, M. H. V.

- Werts, L. Porrès, T. Pons, J. Mertz, S. Tretiak, M. Blanchard-Desce, *J. Phys. Chem. A* **2005**, *109*, 3024–3037; d) F. Terenziani, C. L. Droumaguet, C. Katan, O. Mongin, M. Blanchard-Desce, *ChemPhys-Chem* **2007**, *8*, 723–734; e) J. C. Collings, S.-Y. Poon, C. L. Droumaguet, M. Charlot, C. Katan, L.-O. Palsson, A. Beeby, J. A. Mosely, H. M. Kaiser, D. Kaufmann, W.-Y. Wong, M. Blanchard-Desce, T. B. Marder, *Chem. Eur. J.* **2009**, *15*, 198–208; f) F. Terenziani, V. Parthasarathy, A. Pla-Quintana, T. Maishal, A.-M. Caminade, J.-P. Majoral, M. Blanchard-Desce, *Angew. Chem. Int. Ed.* **2009**, *48*, 8691–8694; *Angew. Chem.* **2009**, *121*, 8847–8850.
- [5] a) M. Drobizhev, A. Karotki, A. Rebane, C. W. Spangler, *Opt. Lett.* **2001**, *26*, 1081–1083; b) M. Drobizhev, A. Karotki, Y. Dzenis, A. Rebane, Z. Suo, C. W. Spangler, *J. Phys. Chem. B* **2003**, *107*, 7540–7543; c) M. Drobizhev, A. Rebane, Z. Suo, C. W. Spangler, *J. Lumin.* **2005**, *111*, 291–305; d) M. Drobizhev, F. Meng, A. Rebane, Y. Stepanenko, E. Nickel, C. W. Spangler, *J. Phys. Chem. B* **2006**, *110*, 9802–9814.
- [6] a) K. D. Belfield, A. R. Morales, J. M. Hales, D. J. Hagan, E. W. V. Stryland, V. M. Chapela, J. Percino, *Chem. Mater.* **2004**, *16*, 2267–2273; b) K. D. Belfield, A. R. Morales, B.-S. Kang, J. M. Hales, D. J. Hagan, E. W. Van Stryland, V. M. Chapela, J. Percino, *Chem. Mater.* **2004**, *16*, 4634–4641; c) S. Yao, K. D. Belfield, *J. Org. Chem.* **2005**, *70*, 5126–5132; d) K. D. Belfield, M. V. Bondar, F. E. Hernandez, O. V. Przhonska, *J. Phys. Chem. C* **2008**, *112*, 5618–5622; e) X. Wang, D. M. Nguyen, C. O. Yanez, L. Rodriguez, H.-Y. Ahn, M. V. Bondar, K. D. Belfield, *J. Am. Chem. Soc.* **2010**, *132*, 12237–12239.
- [7] a) Y. Wang, G. S. He, P. N. Prasad, T. Goodson, III, *J. Am. Chem. Soc.* **2005**, *127*, 10128–10129; b) A. Bhaskar, G. Ramakrishna, Z. Lu, R. Twieg, J. M. Hales, D. J. Hagan, E. V. Stryland, T. Goodson, III, *J. Am. Chem. Soc.* **2006**, *128*, 11840–11849; c) A. Bhaskar, R. Guda, M. M. Haley, T. Goodson, III, *J. Am. Chem. Soc.* **2006**, *128*, 13972–13973; d) O. Varnavski, X. Yan, O. Mongin, M. Blanchard-Desce, T. Goodson, III, *J. Phys. Chem. C* **2007**, *111*, 149–162; e) M. Williams-Harry, A. Bhaskar, G. Ramakrishna, T. Goodson, III, M. Imamura, A. Mawatari, K. Nakao, H. Enozawa, T. Nishinaga, M. Iyoda, *J. Am. Chem. Soc.* **2008**, *130*, 3252–3253.
- [8] a) B. A. Reinhardt, L. L. Brott, S. J. Clarson, A. G. Dillard, J. C. Bhatt, R. Kannan, L. Yuan, G. S. He, P. N. Prasad, *Chem. Mater.* **1998**, *10*, 1863–1874; b) R. Kannan, G. S. He, L. Yuan, F. Xu, P. N. Prasad, A. G. Dombroskie, B. A. Reinhardt, J. W. Baur, R. A. Vaia, L.-S. Tan, *Chem. Mater.* **2001**, *13*, 1896–1904; c) R. Kannan, G. S. He, T.-C. Lin, P. N. Prasad, R. A. Vaia, L.-S. Tan, *Chem. Mater.* **2004**, *16*, 185–194; d) S.-J. Chung, K.-S. Kim, T.-C. Lin, G. S. He, J. Swiatkiewicz, P. N. Prasad, *J. Phys. Chem. B* **1999**, *103*, 10741–10745; e) T.-C. Lin, G. S. He, P. N. Prasad, L.-S. Tan, *J. Mater. Chem.* **2004**, *14*, 982–991; f) Q. Zheng, G. S. He, P. N. Prasad, *Chem. Mater.* **2005**, *17*, 6004–6011.
- [9] a) H. J. Lee, J. Sohn, J. Hwang, S. Y. Park, H. Choi, M. Cha, *Chem. Mater.* **2004**, *16*, 456–465; b) Z. Fang, T.-L. Teo, L. Cai, Y.-H. Lai, A. Samoc, M. Samoc, *Org. Lett.* **2009**, *11*, 1–4; c) Z. Fang, X. Zhang, Y.-H. Lai, B. Liu, *Chem. Commun.* **2009**, 920–922; d) Y. Xie, X. Zhang, Y. Xiao, Y. Zhang, F. Zhou, J. Qi, J. Qu, *Chem. Commun.* **2012**, *48*, 4338–4340; e) C. Tang, Q. Zheng, H. Zhu, L. Wang, S.-C. Chen, E. Ma, X. Chen, *J. Mater. Chem. C* **2013**, *1*, 1771–1780.
- [10] a) T.-C. Lin, Y.-F. Chen, C.-L. Hu, C.-S. Hsu, *J. Mater. Chem.* **2009**, *19*, 7075–7080; b) T.-C. Lin, W.-L. Lin, C.-M. Wang, C.-W. Fu, *Eur. J. Org. Chem.* **2011**, 912–921; c) T.-C. Lin, Y.-H. Lee, C.-Y. Liu, B.-R. Huang, M.-Y. Tsai, Y.-J. Huang, *Chem. Eur. J.* **2013**, *19*, 749–760; d) T.-C. Lin, M.-H. Li, C.-Y. Liu, J.-H. Lin, Y.-K. Shen, Y.-H. Lee, *J. Mater. Chem. C* **2013**, *1*, 2764–2772; e) T.-C. Lin, F.-L. Guo, M.-H. Li, C.-Y. Liu, *Chem. Asian J.* **2013**, *8*, 2102–2110.
- [11] a) C. Bosshard, R. Spreiter, P. Günter, R. R. Tykewski, M. Schreiber, F. Diederich, *Adv. Mater.* **1996**, *8*, 231–234; b) U. Gubler, R. R. Spreiter, C. Bosshard, P. Günter, R. R. Tykewski, F. Diederich, *Appl. Phys. Lett.* **1998**, *73*, 2396–2398; c) F. Diederich, *Chem. Commun.* **2001**, 219–227; d) A. Sune Andersson, K. Qvortrup, E. R. Torbensen, J.-P. Mayer, J.-P. Gisselbrecht, C. Boudon, M. Gross, A. Kadziola, K. Kilså, M. B. Nielsen, *Eur. J. Org. Chem.* **2005**, 3660–3671; e) A. S. Andersson, L. Kerndrup, A. Ø. Madsen, K. Kilså, M. B. Nielsen, P. R. La Porta, I. Biaggio, *J. Org. Chem.* **2009**, *74*, 375–382.
- [12] a) T.-C. Lin, W. Chien, C.-Y. Liu, M.-Y. Tsai, Y.-J. Huang, *Eur. J. Org. Chem.* **2013**, 4262–4269; b) T.-C. Lin, C.-Y. Liu, M.-H. Li, Y.-Y. Liu, S.-Y. Tseng, Y.-T. Wang, Y.-H. Tseng, H.-H. Chu, C.-W. Luo, *J. Mater. Chem. C* **2014**, *2*, 821–828.
- [13] a) M. Parent, O. Mongin, K. Kamada, C. Katan, M. Blanchard-Desce, *Chem. Commun.* **2005**, 2029–2031; b) C. Le Droumaguet, O. Mongin, M. H. V. Werts, M. Blanchard-Desce, *Chem. Commun.* **2005**, 2802–2804; c) F. Terenziani, A. Painelli, C. Katan, M. Charlot, M. Blanchard-Desce, *J. Am. Chem. Soc.* **2006**, *128*, 15742–15755; d) A. Painelli, F. Terenziani, Z. G. Soos, *Theor. Chem. Acc.* **2007**, *117*, 915–931.
- [14] C. Liu, K.-C. Tang, H. Zhang, H.-A. Pan, J. Hua, B. Li, P.-T. Chou, *J. Phys. Chem. A* **2012**, *116*, 12339–12348.
- [15] C. Xu, W. W. Webb, *J. Opt. Soc. Am. B* **1996**, *13*, 481–491.
- [16] N. S. Makarov, M. Drobizhev, A. Rebane, *Opt. Express* **2008**, *16*, 4029–4047.
- [17] M. G. Kuzyk, *J. Chem. Phys.* **2003**, *119*, 8327–8334.
- [18] a) R. L. Sutherland, M. C. Brant, J. Heinrichs, J. E. Rogers, J. E. Slagle, D. G. McLean, P. A. Fleitz, *J. Opt. Soc. Am. B* **2005**, *22*, 1939–1948; b) B. Gu, K. Lou, H.-T. Wang, W. Ji, *Opt. Lett.* **2010**, *35*, 417–419.
- [19] a) Y. Morel, A. Irimia, P. Najchalski, Y. Kervella, O. Stephan, P. L. Baldeck, C. Andraud, *J. Chem. Phys.* **2001**, *114*, 5391–5396; b) P.-A. Bouit, G. Wetzel, G. Berginc, B. Loiseaux, L. Toupet, P. Feneyrou, Y. Bretonnière, K. Kamada, O. Maury, C. Andraud, *Chem. Mater.* **2007**, *19*, 5325–5335; c) C. Li, K. Yang, Y. Feng, X. Su, J. Yang, X. Jin, M. Shui, Y. Wang, X. Zhang, Y. Song, H. Xu, *J. Phys. Chem. B* **2009**, *113*, 15730–15733; d) Q. Bellier, N. S. Makarov, P.-A. Bouit, S. Rigaut, K. Kamada, P. Feneyrou, G. Berginc, O. Maury, J. W. Perry, C. Andraud, *Phys. Chem. Chem. Phys.* **2012**, *14*, 15299–15307.
- [20] a) M. J. Miller, A. G. Mott, B. P. Ketchel, *Proc. SPIE* **1998**, *3472*, 24–29; b) J. S. Shirk, *Opt. Photonics News*, **2000**, *4*, 19–23; c) J. Zhang, Y. Cui, M. Wang, J. Liu, *Chem. Commun.* **2002**, 2526–2527.

Received: February 20, 2014
Published online: April 25, 2014